Electronic Supplementary Material (ESI) for Physical Chemistry Chemical Physics.

Electronic Supplementary Information

Shape-preserving conversion of calcium carbonate tubes to self-propelled micromotors

Qingpu Wang and Oliver Steinbock*

Department of Chemistry and Biochemistry, Florida State University,
Tallahassee, Florida 32306-4390, USA
E-mail: osteinbock@fsu.edu

Table of content

1. ESI figures

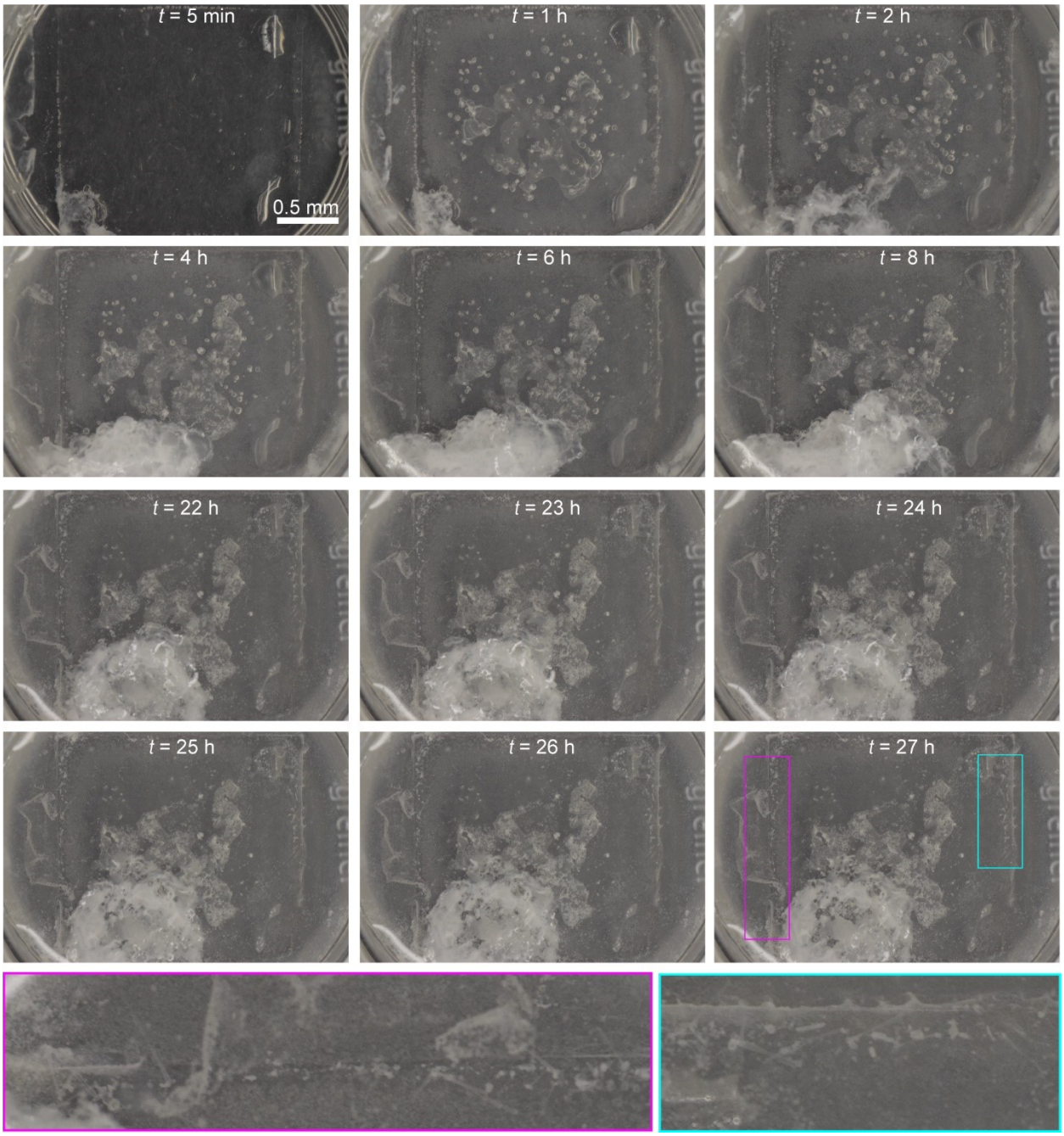

Fig. S1 Photographs showing the growth of precipitate on a Nafion membrane over the course of 27 h. These images were collected from a camera positioned above the Petri dish. The last row shows magnified views from the highlighted areas in the last image (t = 27 h) showing microtubes near the edges of the Nafion membrane.

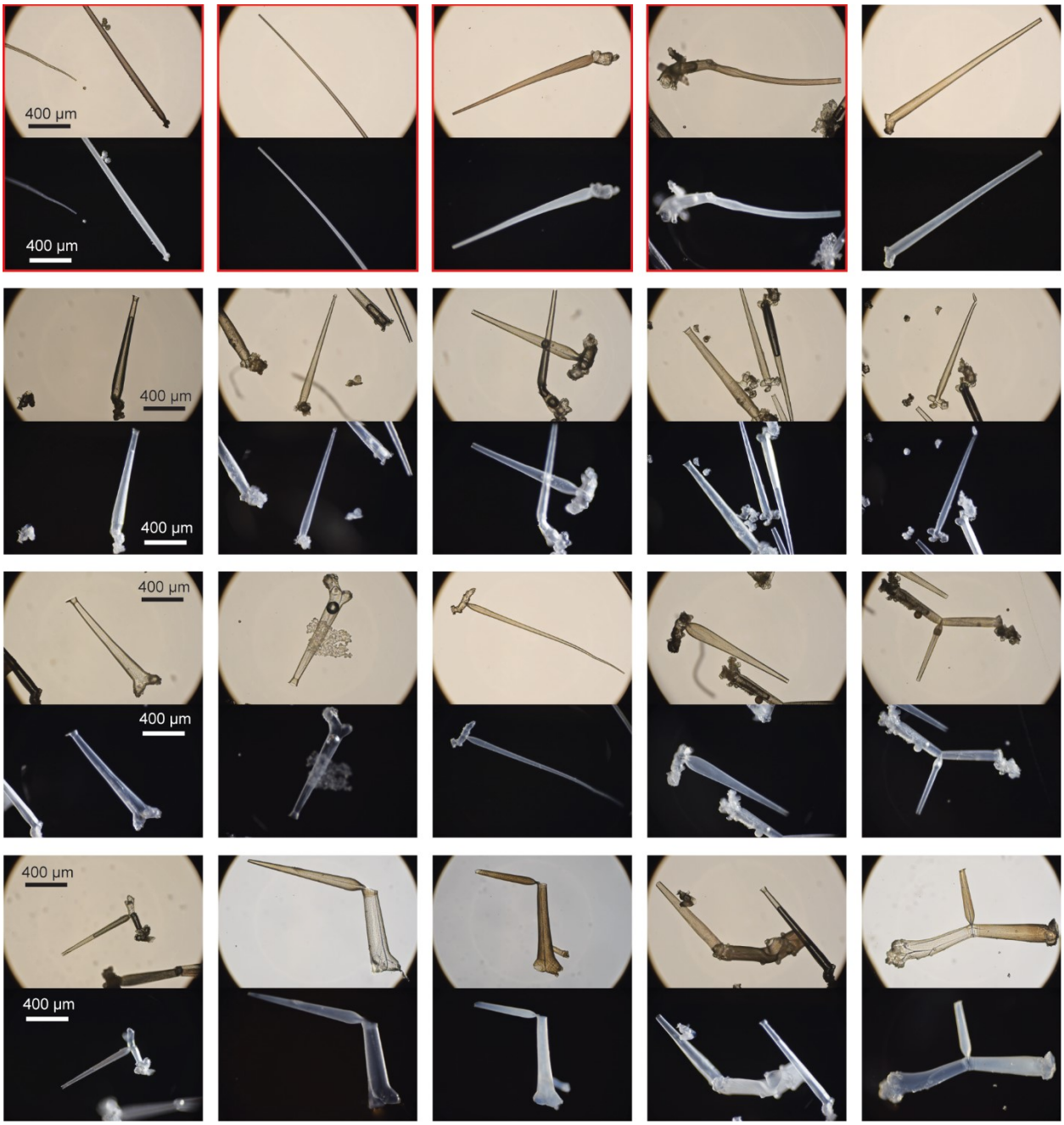

Fig. S2 Optical micrographs of freshly prepared $CaCO_3$ tubes. The image pairs are obtained under transmitted (upper) and dark-field-like (lower) illumination. Images with red borders show calcite tubes, whereas the other examples depict vaterite tubes. All images are at the same scale.

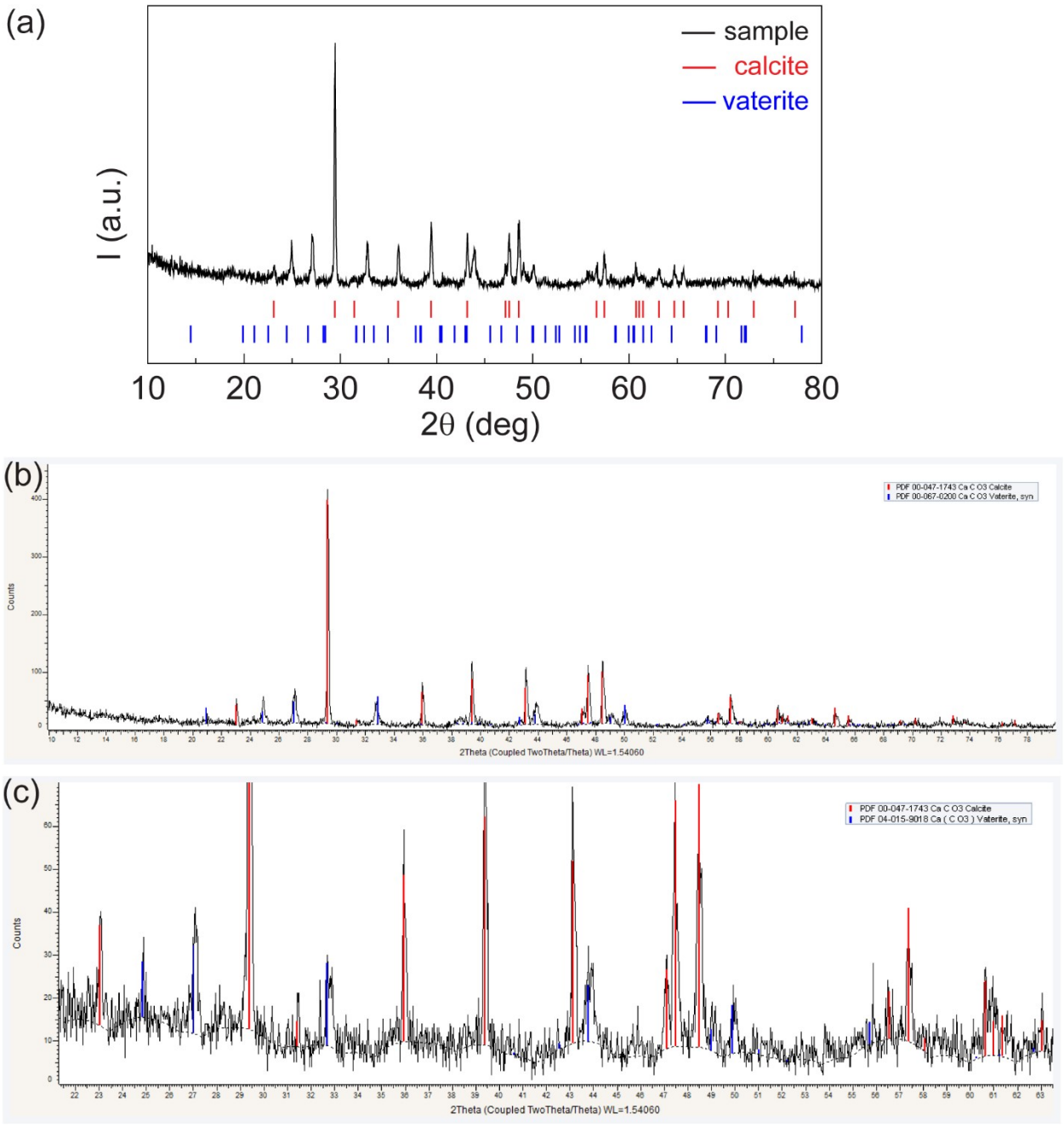

Fig. S3 Powder XRD pattern of the freshly prepared $CaCO_3$ tubes. The red and blue lines indicate reported peak positions for calcite and vaterite according to ref. 16. (b,c) Screenshots from XRD data analysis software (DIFFRAC.EVA) showing a small shift of the vaterite peaks.

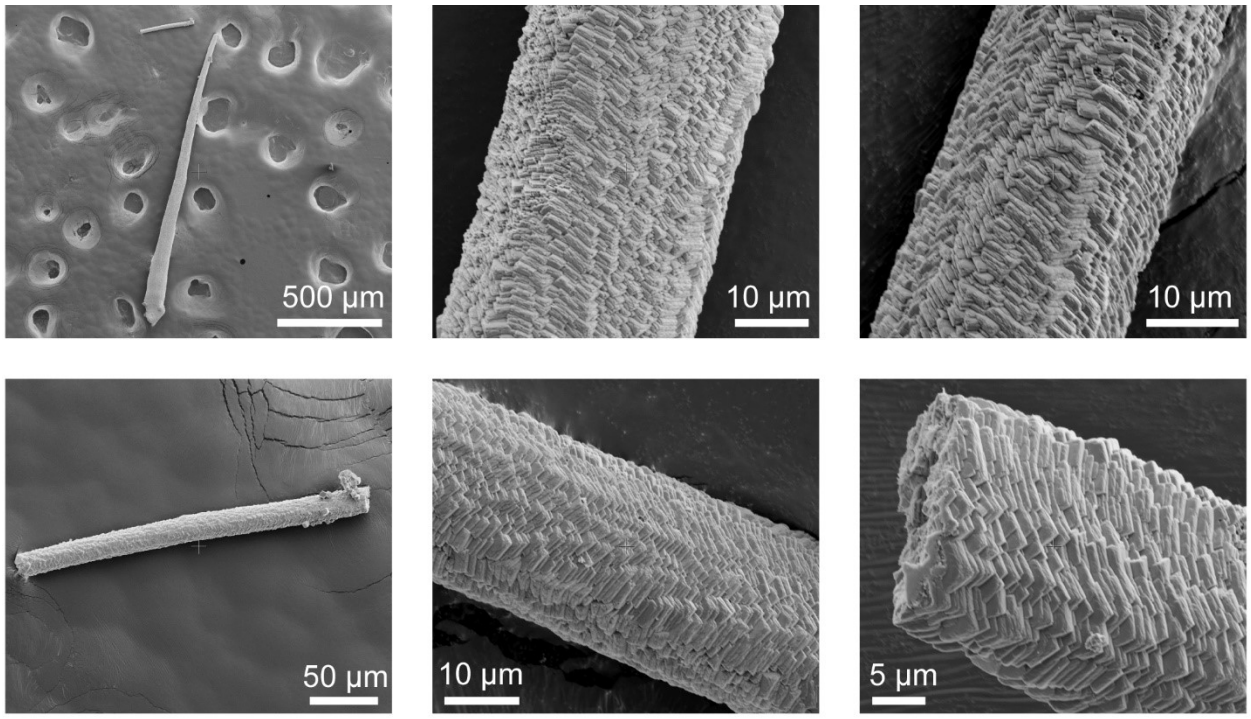

Fig. S4 SEM images of calcite tubes.

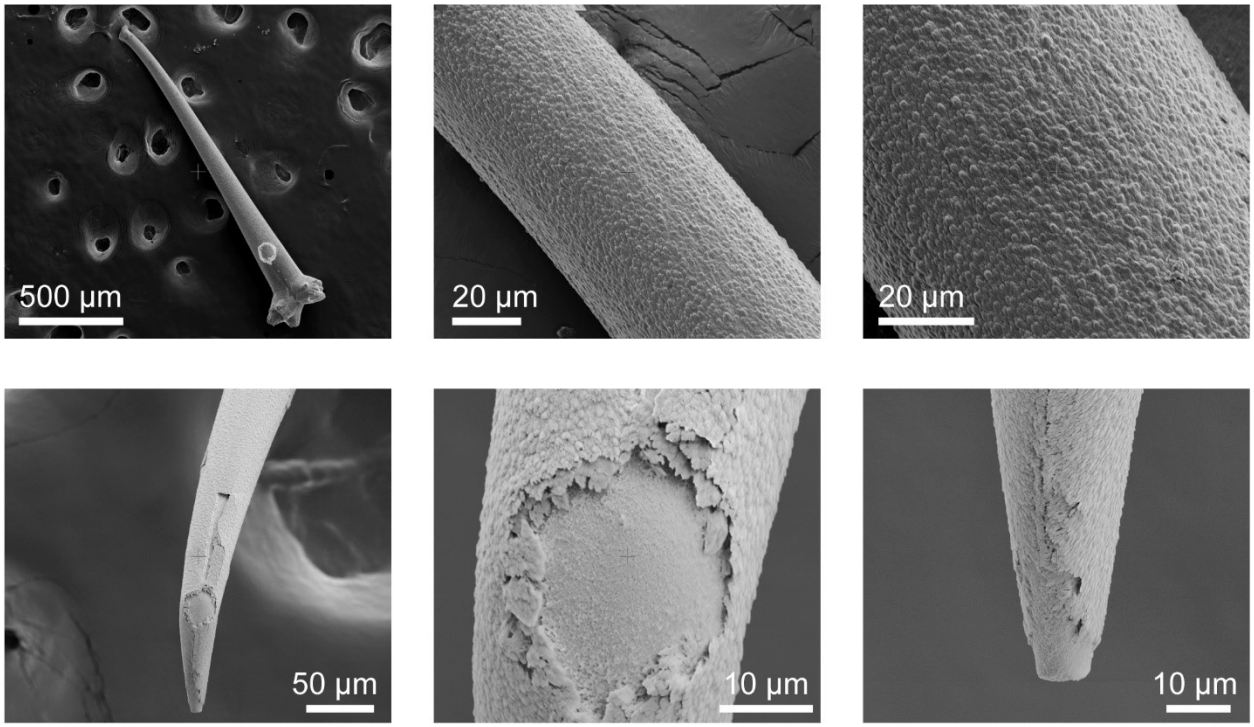

Fig. S5 SEM images of vaterite tubes.

Fig. S6 Optical micrographs of converted tubes. The conversion times are shown left of each image row. The images were obtained by transmitted light microscopy. Scale bar applies to all frames.

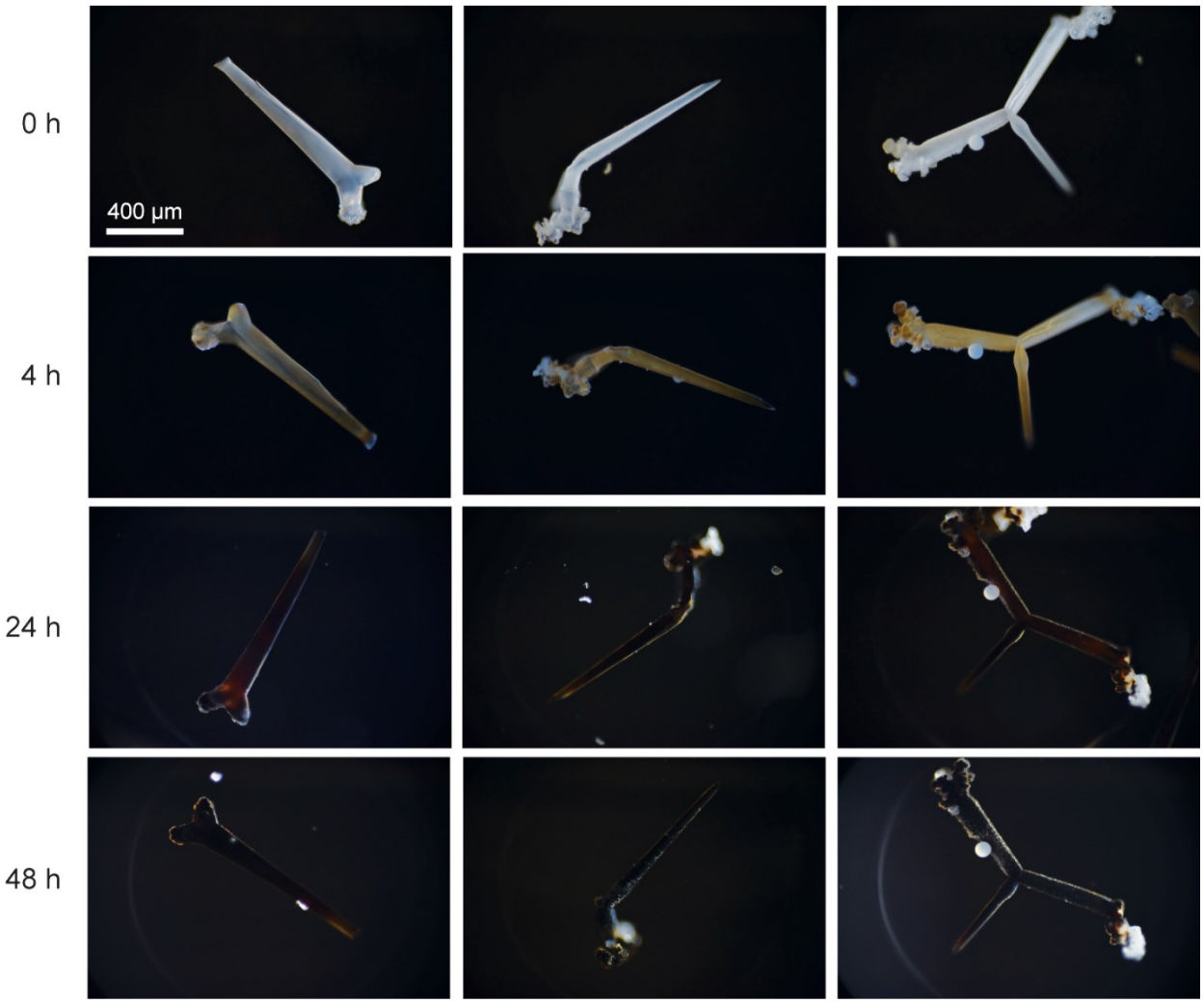

Fig. S7 Optical micrographs of converted tubes. The images were obtained under dark-field illumination. These tubes are the same as the ones shown in Fig. S5. Note that the white tubes become brownish black and lose transparency over time. Scale bar applies to all frames.

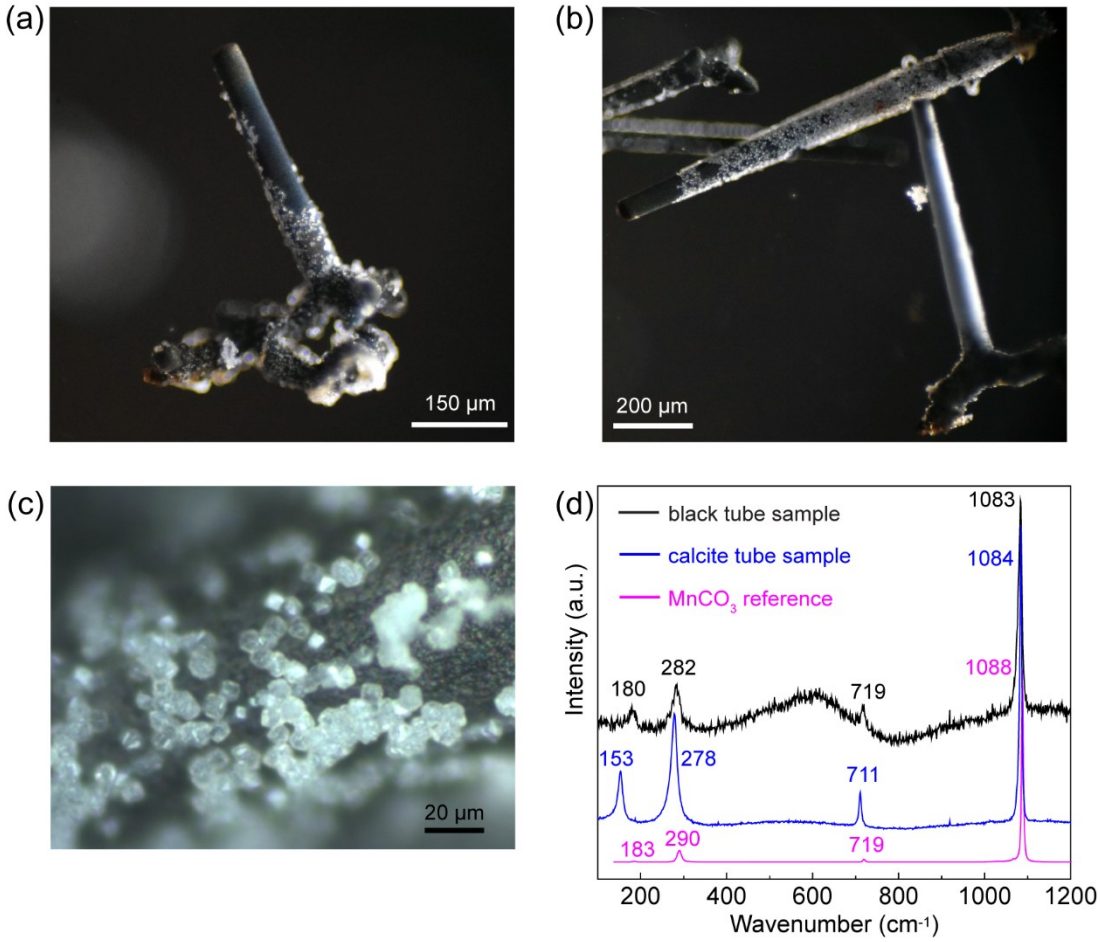

Fig. S8 (a,b) Optical micrographs showing cubic crystals on a converted black tube under reflected light. (c) Optical micrograph of the sample area used to collect the micro-Raman spectrum in (d). The magenta curve is a reference Raman spectrum of $MnCO_3$ (RRUFF ID: R040133). The blue curve is the spectrum of a fresh calcite tube. The sharp peak of the black tube sample at 1083 cm^{-1} matches the calcite peak at 1084 cm^{-1}. The peak at 719 cm^{-1} matches the $MnCO_3$ peak. The two low-frequency peaks at 180 and 128 cm^{-1} are close to the $MnCO_3$ peak at 180 cm^{-1} and the calcite peak at 278 cm^{-1}. Thus, the micro-Raman measurement indicates the sample contains at least calcite $CaCO_3$ and $MnCO_3$. The broad, low-intensity peak around 600 cm^{-1} might be attributed to Mn oxides because an earlier study[1] reported varying peak positions around 600 cm^{-1} for seven different Mn oxides.

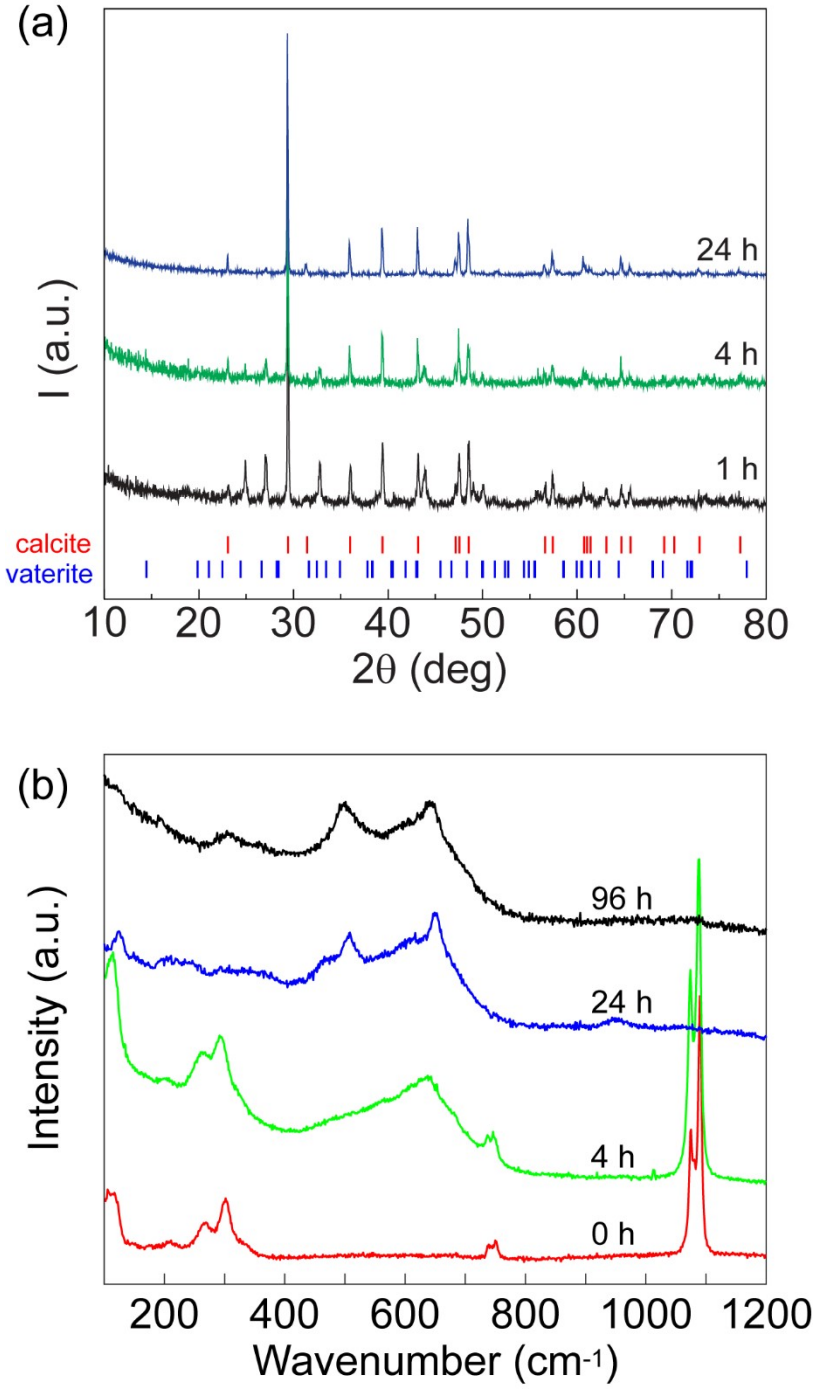

Fig. S9 (a) Powder XRD patterns of the same sample with different exposure times to the $MnCl_2$ solution. These data are the same as those shown in Fig. 2h but extend to 2θ = 80 degrees. (b) Micro-Raman spectra of vaterite tubes obtained from experiments with different exposure times to the $MnCl_2$ solution. The peaks at 501 and 635 cm^{-1} in the spectrum at 96 h might be attributed to Mn oxides[1]. We note that the room-temperature conversion of $MnCO_3$ to Mn oxides has been previously reported[2].

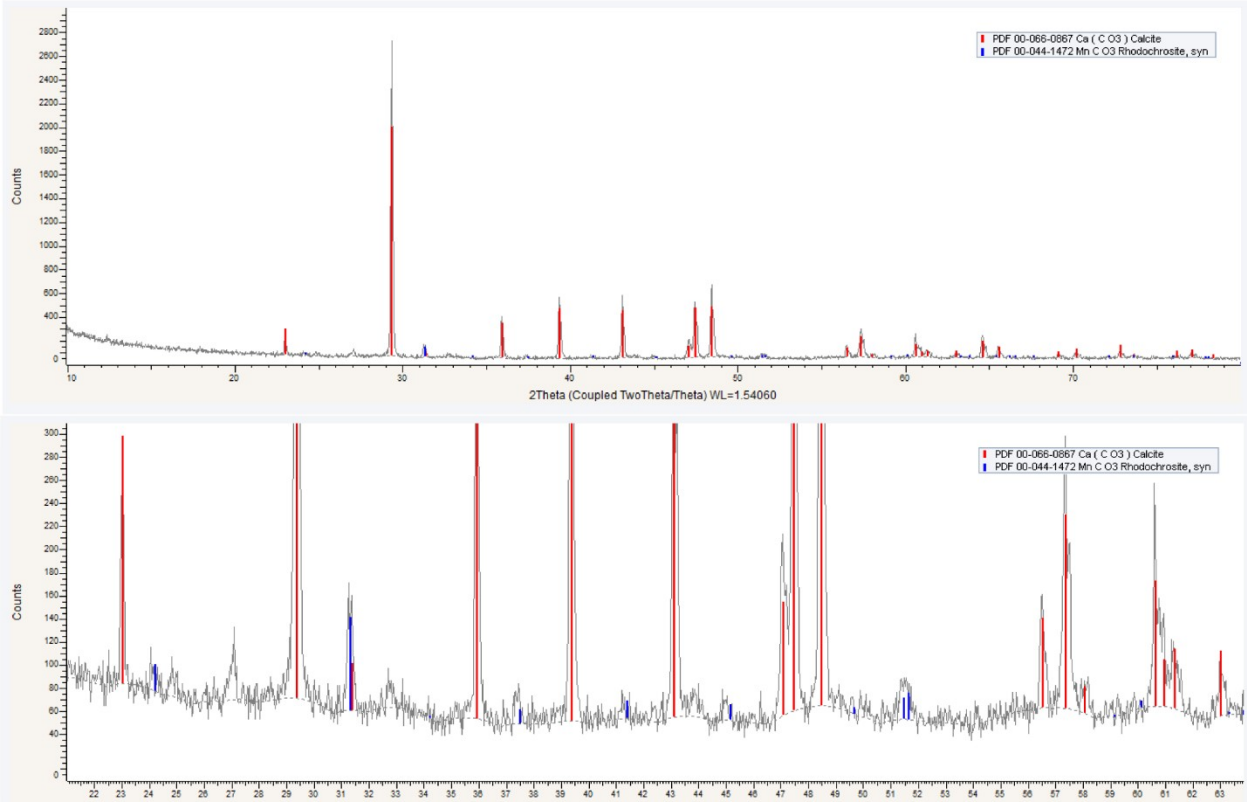

Fig. S10 Analysis of the XRD pattern in Fig. S9a at 24 h with the full range (upper panel) and a magnified view (lower panel). The results show characteristic peaks of $MnCO_3$The peak heights are much lower than those of calcite indicating a low compositional percentage.

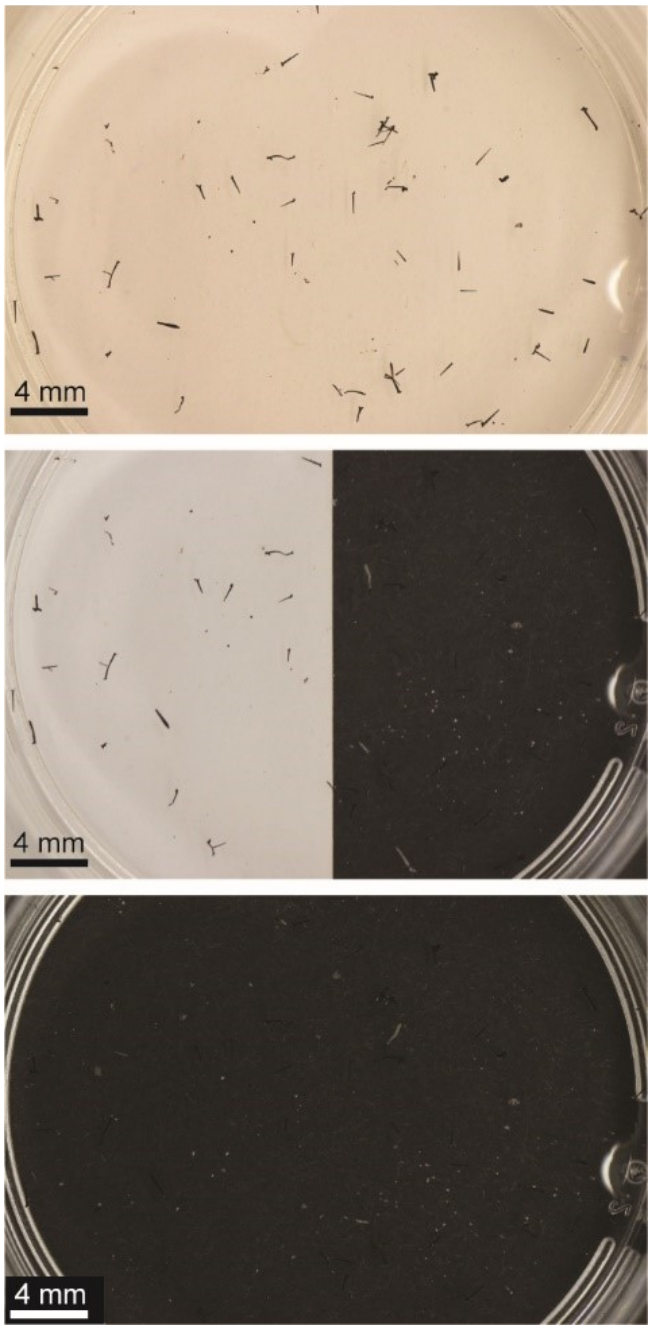

Fig. S11 Photographs of $CaCO_3$ tubes after 3 days in 10 mM $MnCl_2$ illustrating that some fraction of the tube population did not convert. Also see Movie S1.

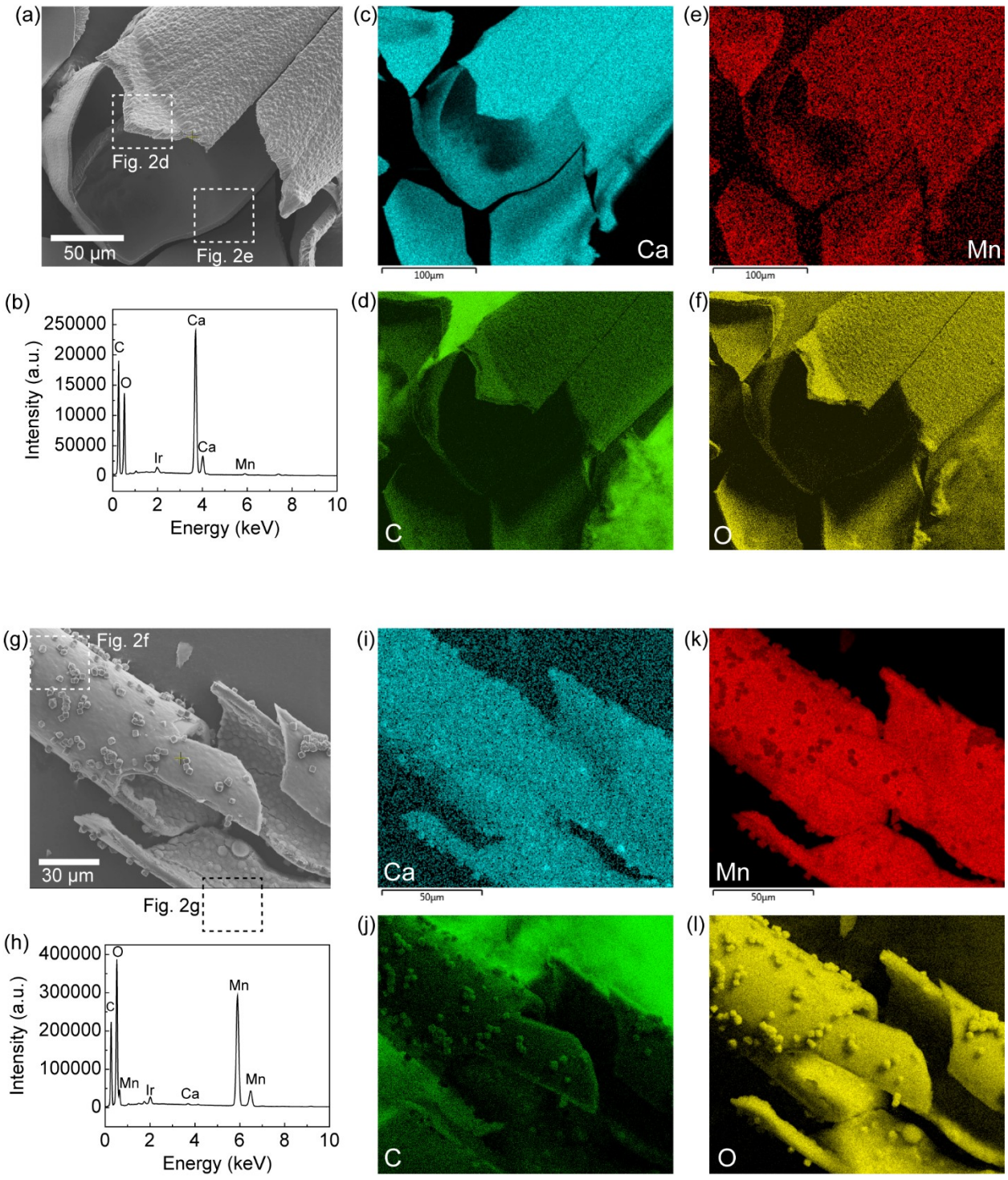

Fig. S12 SEM and EDS measurement of a brown tube (a-f) and a black tube (g-l). The boxes in (a,g) indicate the approximate areas for which the SEM images in Figs. 2d-g were collected. The EDS spectra in (b,h) are map sum spectra obtained from the entire scan area of the images. The weight percentages of Ca and Mn are 97.1%, 2.9 % (c,e) and 0.4%, 99.6 %(I,k), respectively.

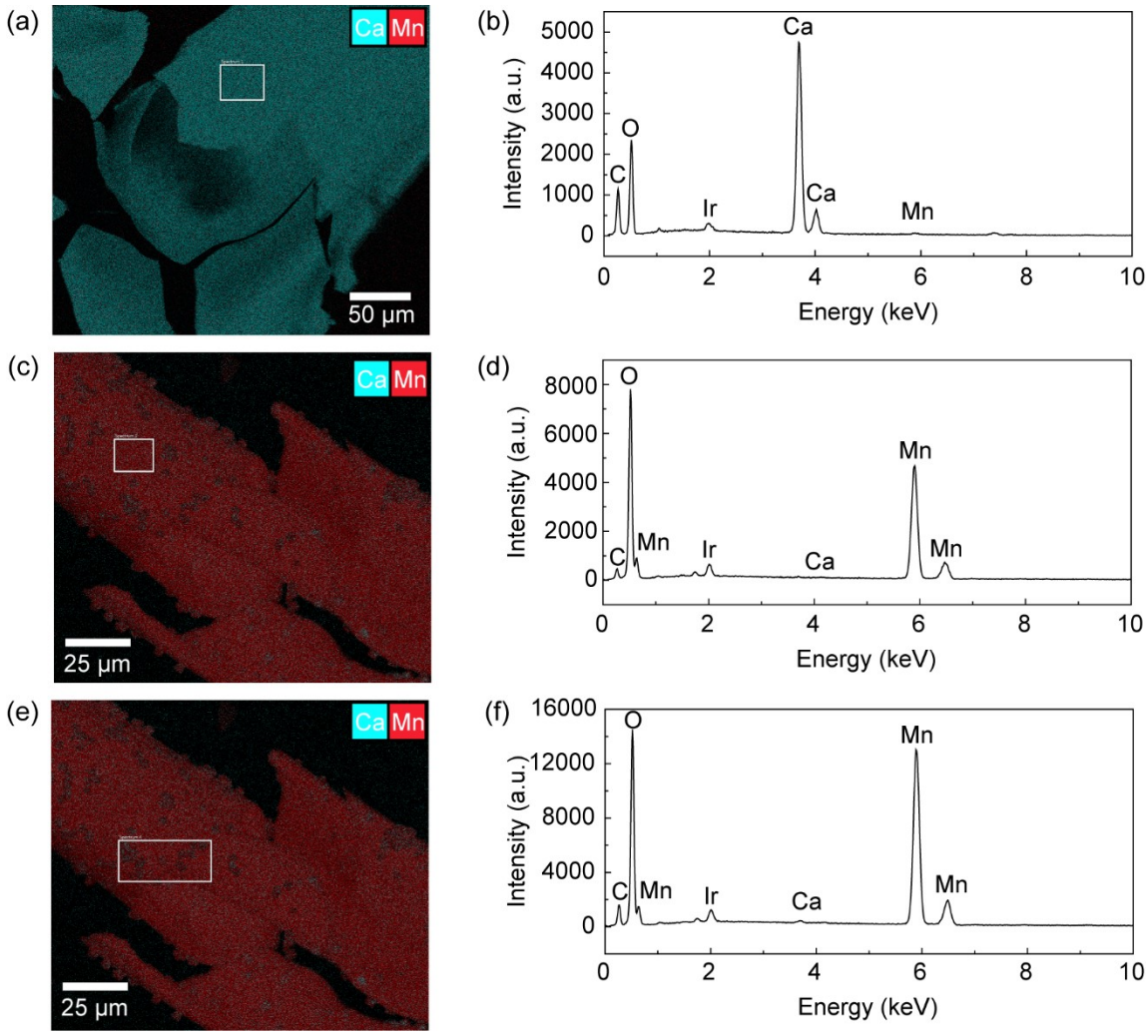

Fig. S13 EDS TruMap images of a brown tube (a) and a black tube (c,e). Note that the color intensities in these images display the real variation of X-rays from the elements in the specimen, and therefore, represent the absolute amount of elements detected. In comparison, the color intensities in Fig. S10 are automatically normalized for each element. (b,d,f) EDS spectra of selected rectangular areas in (a,c,e), respectively. The selected areas are indicated by white boxes in (a), (c), and (e).

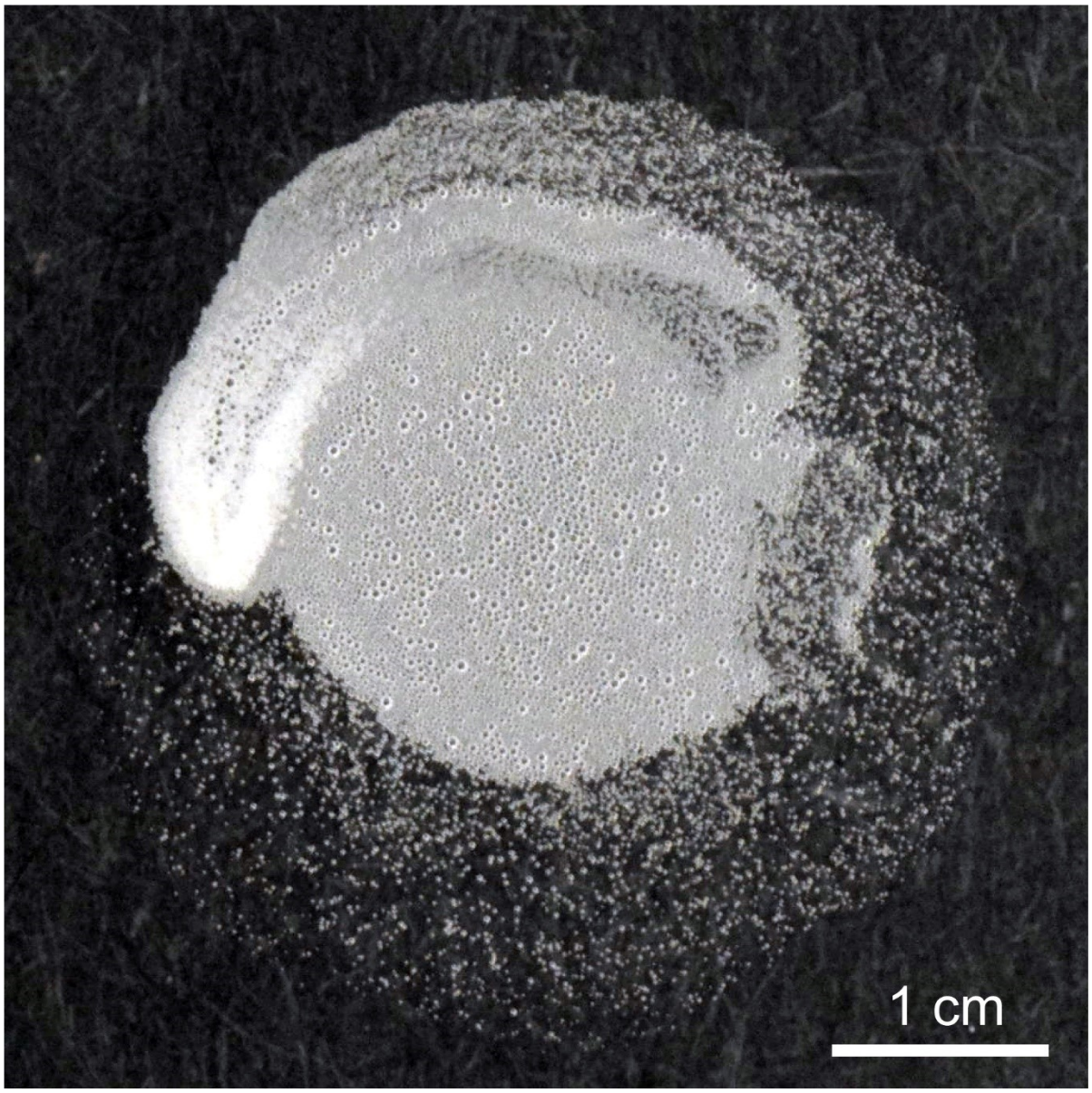

Fig. S14 Photograph of the foam-like pattern formed by a tube in 0.5 mM AOT and 2% H_2O_2 solution after 7 min. This image provides a magnified view for the experiment in Fig. 3a (top row).

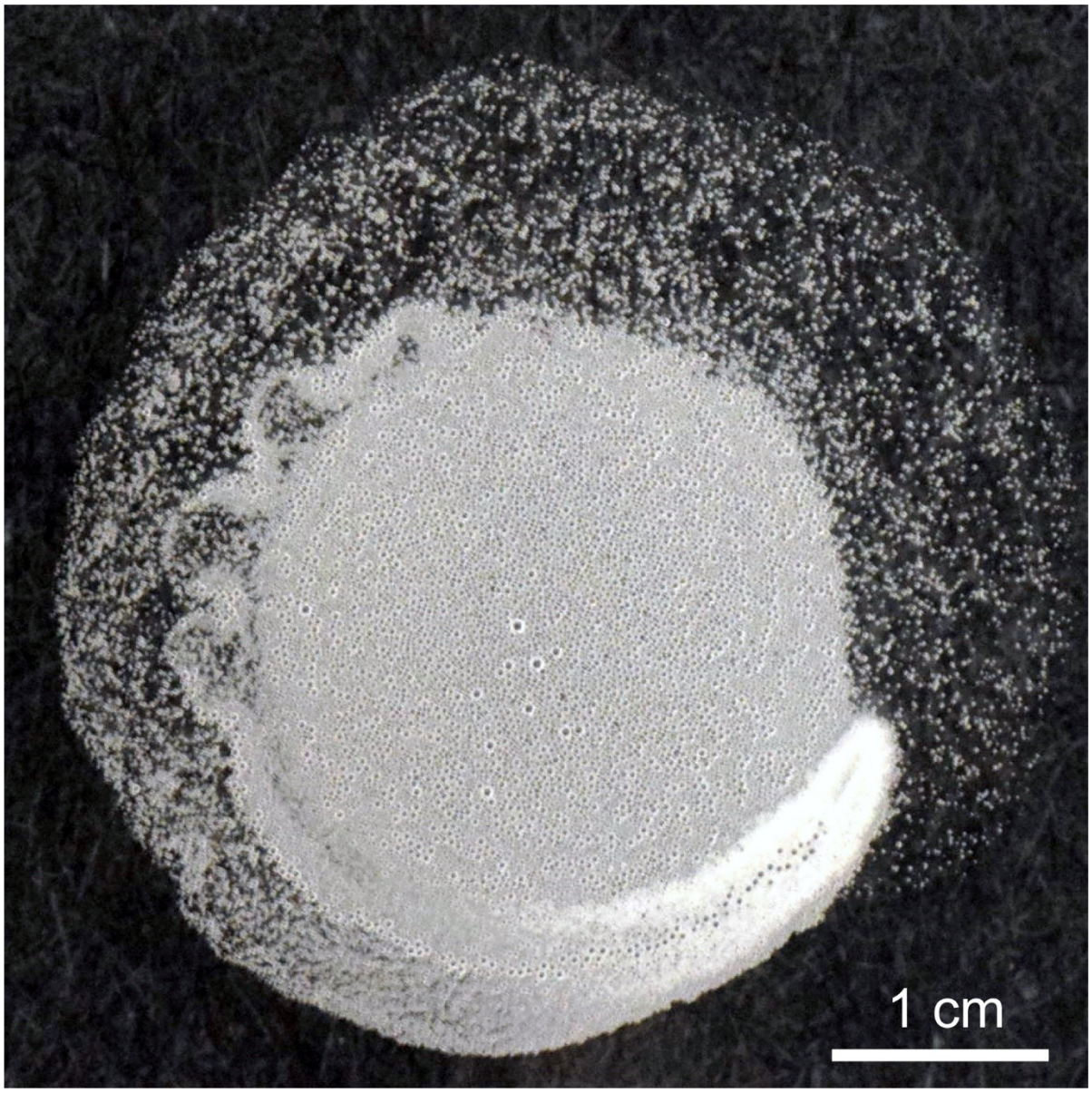

Fig. S15 Photograph of the foam-like pattern formed by a tube in 1.0 mM AOT and 2% H_2O_2 solution after 18 min. The tube in this experiment is the same as the one in Fig. S11. This image complements the information in Fig. 3a by showing the foam pattern observed at a higher AOT concentration.

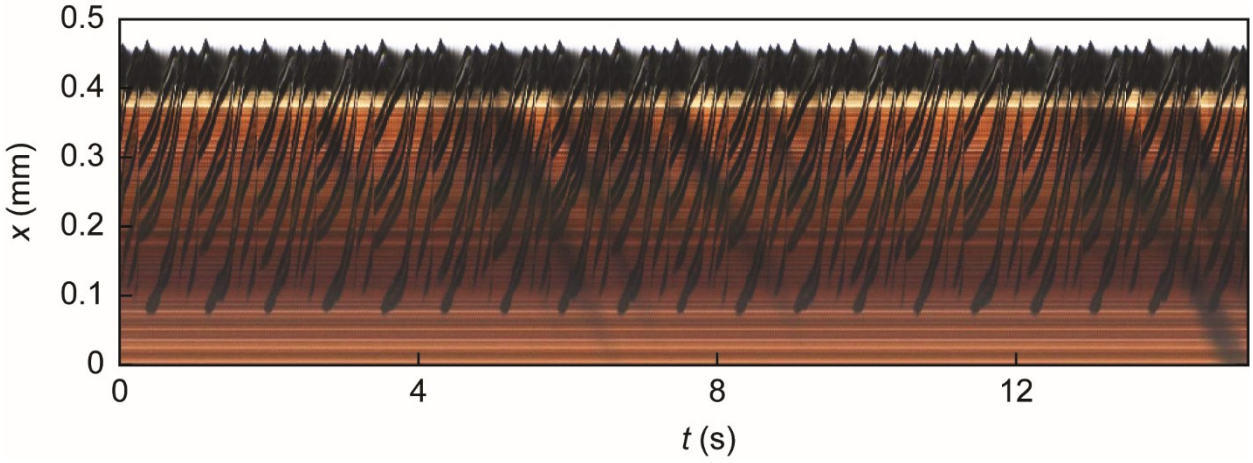

Fig. S16 Time-space plot illustrating the nucleation and movement of bubbles within a transparent conical tube submerged in 0.05% H_2O_2. The plot extends over 16 s of which the first 3 s are identical to Fig. 3b.

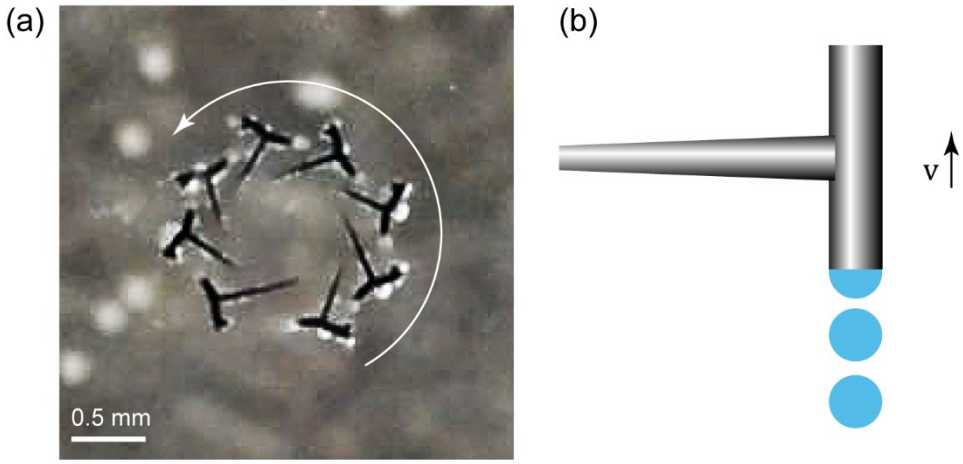

Fig. S17 (a) Superimposed images containing eight consecutive frames with an interval of 20 ms. See also Movie S5. (b) Schematics of the bubble-driven motion of this type of T-shaped tube.

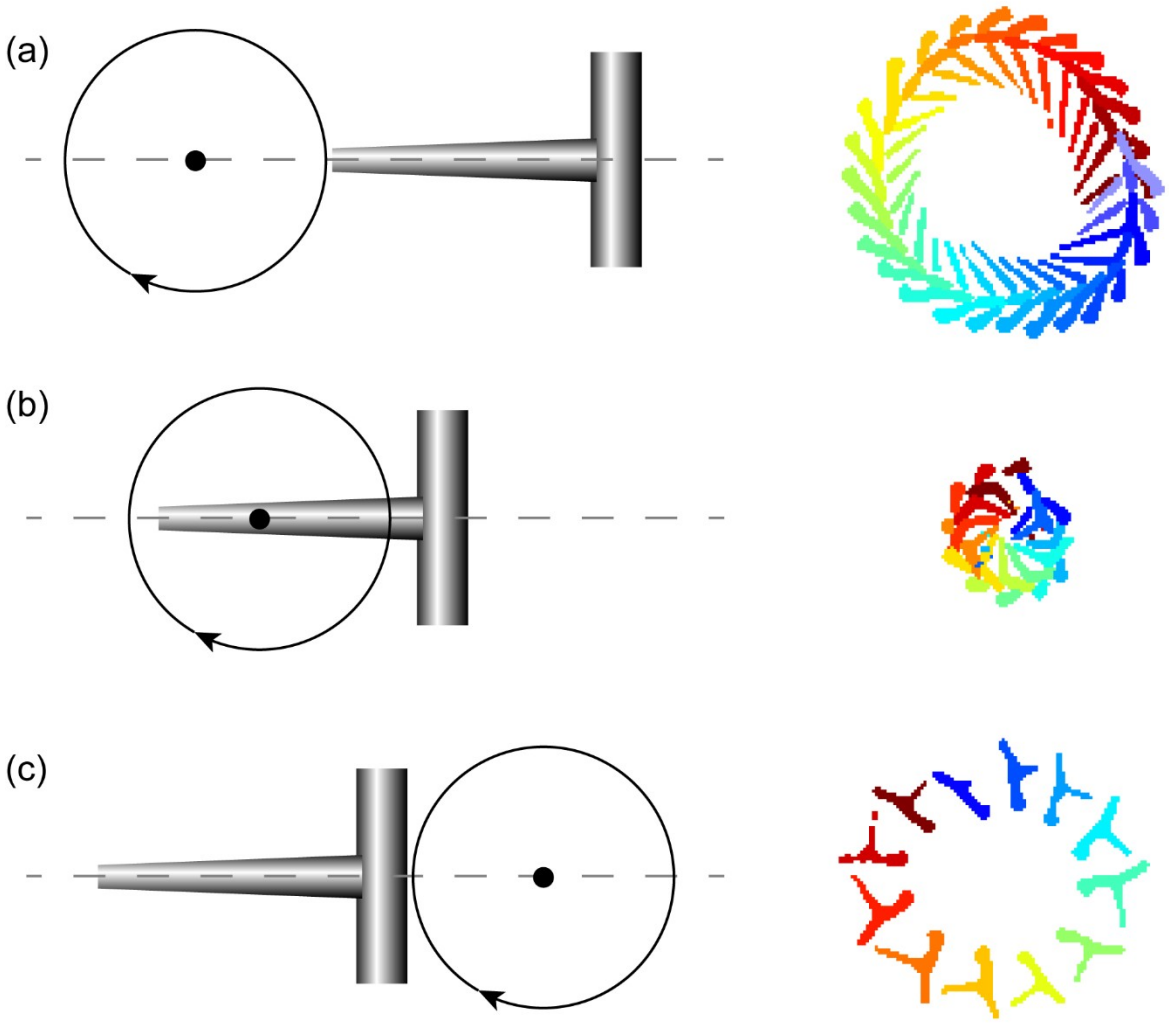

Fig. S18 Most T-shaped tubes revolve around a only slowly drifting center point without any superposed spinning motion. The distance between the tube and this point determines the resulting motion pattern. The examples shown here highlight a center point off the T stem (a), on the stem (b), and off the bar of the T-shape (c). The color maps in the right column are experimental data for which tube positions were superposed and color-coded according to time (blue early, red late).

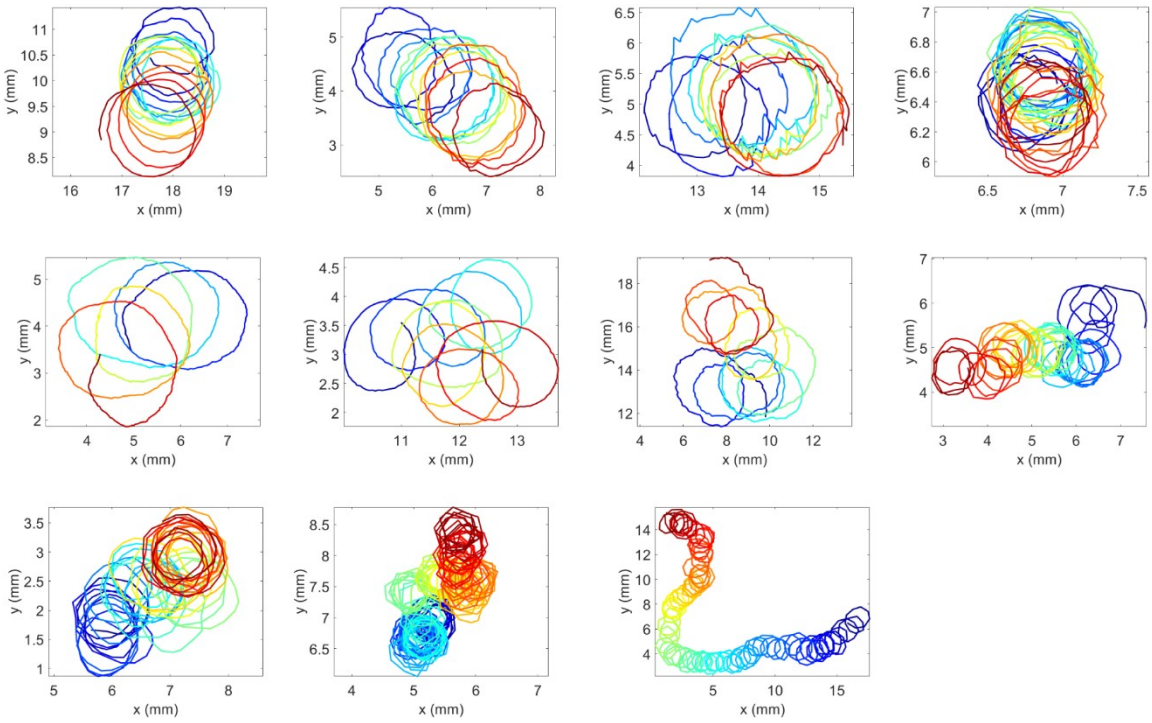

Fig. S19 Long-term evolution of the trajectories of T-shaped tubes complementing the example shown in Fig. 4b. The trajectories result from the slow drift of the center point in Fig. S15 that causes the circular trajectory to transform into various tightly wound patterns. These plots were obtained from five different T-shaped tubes in H_2O_2 concentrations between 1% and 9% w/v.

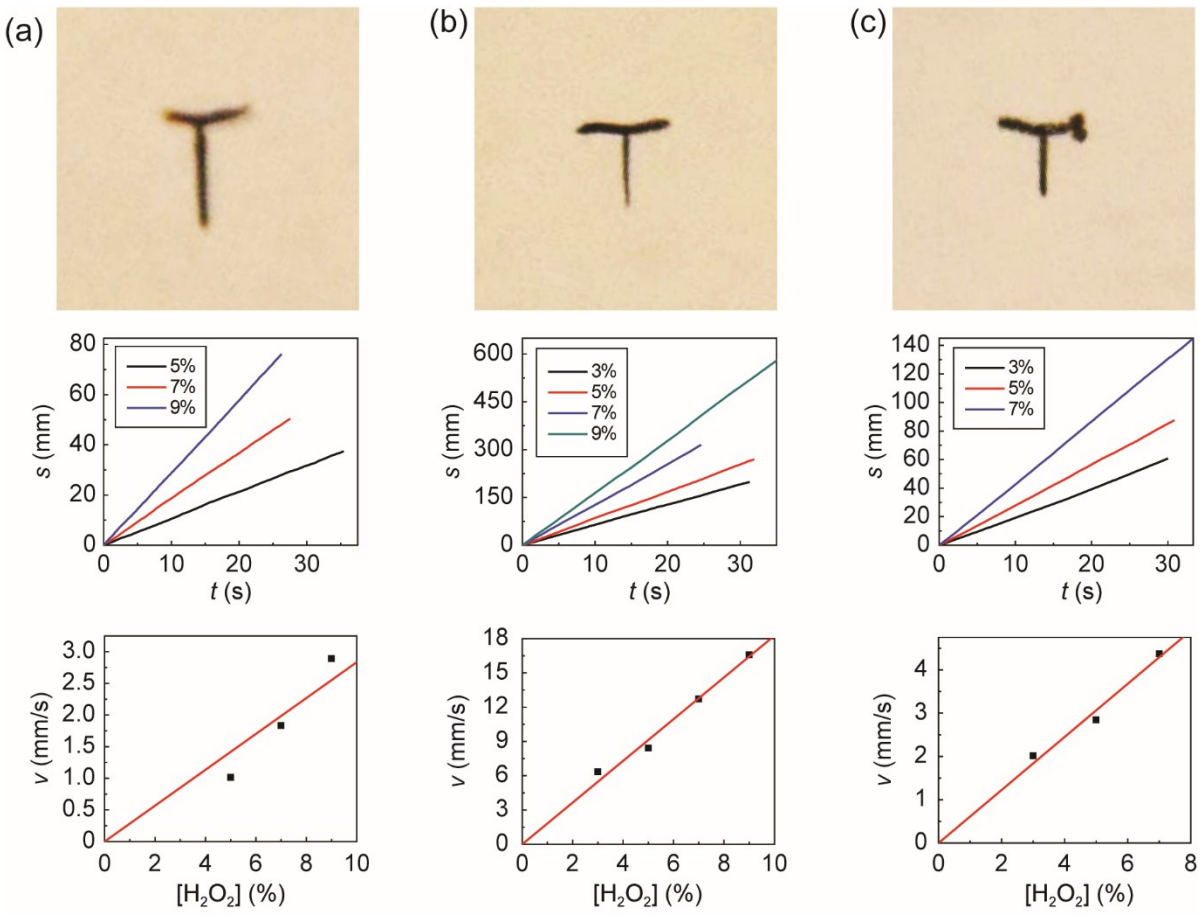

Fig. S20 Tube velocity as a function of H_2O_2 concentration for three different T-shaped tubes. The red lines in the lowest row are proportional fits with proportionality constants of 0.86 (a), 5.6 (b), and 1.9 mm L/(s mol) (c). Notice that the H_2O_2 concentration was converted to mol/L. Field of view: 2 × 2 mm^2.

2. ESI movies

Movie S1. Time-lapse video based on optical micrographs showing the conversion process of a conical vaterite tube.

Movie S2. Time-lapse movie showing a chemical garden tube during a three-day shape-preserving conversion. This movie also supports our finding that the white color of some tubes remained unchanged.

Movie S3. Time-lapse movie showing self-propelled Ca-to-Mn converted tubes undergoing self-motion in 2% H_2O_2 solutions containing 0, 0.1, and 0.5 mM AOT.

Movie S4. Real-time movie showing the rhythmic nucleation, growth, and release of bubbles in a stationary conical tube.

Movie S5. Real-time movie showing a T-shaped tube in 3% H_2O_2 solution.

3. ESI references

1 Y. Xin, H. Cao, C. Liu, J. Chen, P. Liu, Y. Lu, and Z. Ling, *J. Raman Spectrosc.,* 2022, **53**, 340-355.

2 X. Zhang, P. Yu, D. Zhang, H. Zhang, X. Sun, and Y. Ma, *Mater. Lett.*, 2013, **92**, 401-404.